

# Color Visualization System for Near-Infrared Multispectral Images

*Meritxell Vilaseca<sup>1</sup>, Jaume Pujol<sup>1</sup>, Montserrat Arjona<sup>1</sup>,  
and Francisco Miguel Martínez-Verdú<sup>2</sup>*

*<sup>1</sup>Center for Sensors, Instruments and Systems Development (CD6)*

*Dept. of Optics and Optometry, Technical University of Catalonia, Terrassa, Spain*

*<sup>2</sup>Department of Optics, University of Alicante, Alicante, Spain*

## Abstract

In this paper, we analyze a color visualization system for multispectral images belonging to the near-infrared region (NIR, 800-1000 nm). Samples with the same appearance in the visible region can differ in the NIR and can be differentiated by taking into account the extra information included in this region. Using a multispectral system, five different images of textile samples with varying spectral reflectance are obtained. The aim of the study is to analyze how the monochromatic images or spectral bands of the samples (with only a few shades of gray) should be combined in order to obtain a false pseudocolored image (with a large range of different colors). With the color image, it is possible to discriminate clearly between different objects. In order to achieve this separation, it is necessary to define a color space representation. In this paper, several possible combinations based on different methods are presented. The pseudocolored images are then visualized on a calibrated CRT monitor. Finally, the color differences between samples are evaluated using several parameters. The methods which provide the best results in terms of visual discrimination are based on PCA analysis.

## Introduction

The aim of this study is to develop a color visualization system for multispectral images belonging to the NIR region of the spectrum<sup>1</sup>. This spectral range can contain information related to the chemical properties of the objects, and therefore samples with the same appearance in the visible region can differ in the NIR and may be differentiated by taking into account the extra information provided. This can be useful in several fields, such as in the textile and chemical industries, military applications, etc.

The process used in this study can be divided into the following two main stages:

1. **Pseudocolorimetry Definition.** Using five monochromatic images of the samples analyzed (twenty-five textile samples), which correspond to different spectral bands of the NIR obtained with a multispectral system developed for this region,<sup>1</sup> the pseudocolorimetry<sup>2</sup> must be defined in order to generate three signals ( $R_{NIR}$ ,  $G_{NIR}$  and  $B_{NIR}$ ). These values can be considered the pseudocolors of the

samples. In this paper, several color representation methods are proposed.

2. **Calibration of the Visualization Device.** In order to obtain a final pseudocolored image which is independent of the visualization device, the  $R_{NIR}$ ,  $G_{NIR}$  and  $B_{NIR}$  signals must be transformed. For this purpose, it is necessary to calibrate the device used—in our case, a conventional CRT monitor—and to define three new signals called  $R_{Monitor}$ ,  $G_{Monitor}$  and  $B_{Monitor}$ . These signals can be associated with the channels of the monitor.

Subsequent to the two steps described above, analyses of the colorimetric differences of the samples were performed using all the methodologies proposed. Several different parameters, such as contrast levels, CIELAB color differences, etc., were used.

## Method

### 1. Pseudocolorimetry Definition

The experimental setup used in the first stage of the study was a multispectral acquisition system consisting of a monochrome CCD camera with improved response in the NIR region (Hamamatsu C7500-51). This was connected to a frame grabber (Matrox IP8), an illumination system composed of a halogen lamp (Philips 15V 150W), and five equi-spaced interference filters (ThermoCorion) in the region studied, which defined the different spectral acquisition bands (Figure 1). Using this configuration, five different images were obtained, each composed of twenty-five textile samples with different spectral reflectance in the NIR (Figure 2). Subsequently, a pseudo-white balance process was performed in order to obtain equal responses through all channels for a sample with a constant spectral reflectance. The digital responses were limited from 0 to 255 (8 bits).

Once the five monochrome images had been captured, it was necessary to define a color representation to obtain a single pseudocolored image with a large range of different colors and therefore a high level of discrimination between samples. Basically, the pseudocoloring methods used in these studies may be classified into the following two groups: methods for simulating the color vision of the human eye and methods for maximum colorimetric discrimination. The first type of method attempts to

simulate the color vision that the human eye has in the visible range in the NIR region. The second type includes methods which increase colorimetric discrimination between objects, without taking into account the color vision of the human eye.

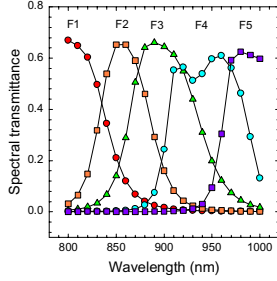


Figure 1. Interference filters of the NIR multispectral system

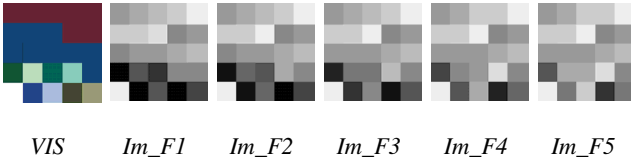


Figure 2. Visible image and five NIR monochromatic images of the twenty-five textile samples

As an initial approximation to the first type of method, we used simple combinations by directly associating several of the multispectral monochromatic images to the signals  $R_{NIR}$ ,  $G_{NIR}$  and  $B_{NIR}$ . The images or spectral bands corresponding to long wavelengths were associated with red; medium wavelengths with green and short wavelengths with blue. An example might be the following:

$$\begin{aligned} R_{NIR} &= 0.5 \text{Im}_F4 + 0.5 \text{Im}_F5 \\ G_{NIR} &= \text{Im}_F3 \\ B_{NIR} &= 0.5 \text{Im}_F1 + 0.5 \text{Im}_F2 \end{aligned} \quad (1)$$

where  $\text{Im}_F_i$  ( $i = 1, \dots, 5$ ) are the NIR monochromatic images obtained for the different spectral bands.

A more complex method is to display a carefully selected combination of the monochromatic images that account for the  $RGB$  responses of the CIE-1931 standard observer, that is, the tristimulus values defined in this color space. Translating and compressing the color-matching functions of this space into the analyzed range is necessary in order to obtain behavior in the NIR which is equivalent or similar to that of the visible region. The pseudocolor matching functions in the NIR must be approximated from a combination of the transmittance of the five filters used. This was performed using a least squares regression (Figure 3). As shown, the original and approximated functions differed considerably.

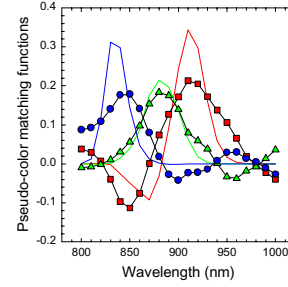


Figure 3. Pseudocolor matching functions in the NIR region (line curves represent original functions and dotted curves represent simulated functions).

In addition to the two methods described so far, other typical color appearance models<sup>3,4</sup> used in the visible region can be translated into the NIR region, such as *LMS* models (cone excitation space) and *ATD* models (neural or zone models). *LMS* models simulate the response for each type of photoreceptor and calculate the quantities  $L$ ,  $M$  and  $S$  using the tristimulus values of the CIE-1931 standard observer. These values can be associated with the  $R_{NIR}$ ,  $G_{NIR}$  and  $B_{NIR}$  signals. Equation (2) is an example that uses the Hurvich-Jameson model:

$$\begin{bmatrix} L \\ M \\ S \end{bmatrix} = \begin{bmatrix} 11.63 & 30.00 & 1.12 \\ 11.37 & 31.80 & 0.41 \\ 0.33 & 30.01 & -0.39 \end{bmatrix} \begin{bmatrix} R \\ G \\ B \end{bmatrix} \quad (2)$$

In our case, the  $R$ ,  $G$  and  $B$  signals are the approximated tristimulus values of the CIE-1931 standard observer in the NIR.

The *ATD* models are used to calculate the *LMS* signals and also to take into account the opponent-colors theory. These models compute three new signals from the *LMS* values:  $A$  is the achromatic signal,  $T$  the red-green signal and  $D$  the yellow-blue signal. Examples include the Hurvich-Jameson model, Guth and cols., Ingling and Tsou., CIELAB, Retinex, the Nayatani model, etc. Using these methods, the signals can be associated with the  $R_{NIR}$ ,  $G_{NIR}$  and  $B_{NIR}$  values as follows:

$$\begin{aligned} R_{NIR} &= A + T \text{ (if } T > 0) + D \text{ (if } D > 0) \\ G_{NIR} &= A + T \text{ (if } T < 0) + D \text{ (if } D > 0) \\ B_{NIR} &= A + D \text{ (if } D < 0) \end{aligned} \quad (3)$$

By way of example, the Hurvich-Jameson model is represented in Equation (4).

$$\begin{bmatrix} A \\ T \\ D \end{bmatrix} = \begin{bmatrix} 0.85 & 1.50 & 0.01 \\ 1.66 & -2.33 & 0.37 \\ 0.34 & 0.06 & -0.71 \end{bmatrix} \begin{bmatrix} L \\ M \\ S \end{bmatrix} \quad (4)$$

Finally, we studied a further method called the red-cyan model,<sup>2</sup> which is based on the opponent-colors theory. According to this model, the monochromatic images corresponding to spectral bands with greater wavelengths are associated with the  $R_{NIR}$  Channel, and images corresponding to shorter wavelengths are simultaneously displayed on the  $G_{NIR}$  and  $B_{NIR}$  Channels, thus giving the cyan color. By means of this combination, samples with high reflectance at long wavelengths appear

reddish and samples with high reflectance at short wavelengths are represented as cyan. A sample with a constant reflectance would appear gray.

Any of the combinations described (methods which simulate the color vision of the human eye) can cause problems due to the high correlation of the different spectral bands which are often present in the NIR region. In order to solve this, we can simply use decorrelation methods that facilitate the colorimetric discrimination between objects and do not simulate the human eye's response. In this case, we first propose using principal component analysis (PCA).<sup>5</sup> By using this method, each pixel can be associated with a vector of five components, which correspond to the gray level of each spectral band. By applying PCA to the set of vectors (i.e. the scene statistics), it is possible to establish a new coordinate system whose axes are in the direction of the eigenvectors, that is, the main directions common to all the pixels of the images. In this way, the mechanism can decorrelate the data. Once the analysis is performed, we can choose the three principal component directions (eigenvectors related to the three largest eigenvalues) and associate them with the  $R_{NIR}$ ,  $G_{NIR}$  and  $B_{NIR}$  signals. With this kind of association, it is possible to assign very different colors to samples with similar reflectance spectra, so problems in terms of color constancy can appear.

In order to overcome this limitation, a transformation of this association can be performed. This transformation (PCA modified method), consists in simultaneously associating the principal component of the scene statistics to the  $R_{NIR}$ ,  $G_{NIR}$  and  $B_{NIR}$  signals. Therefore, this component of the pixels accounts for the brightness. The second and third principal components constitute an orthogonal plane to the brightness direction and can be considered a chromaticity plane. For example, considering the conventional rectangular color representation, the second principal vector can be associated with the red-green direction and the third can be associated with the yellow-blue direction. Thus, if the contribution of the analyzed pixel to the direction of the second principal vector is positive, it can be interpreted as red and, if it is negative, as green. Equivalently, depending on the sign of its component along the third principal direction, it can be interpreted as yellow or blue (Figure 4).

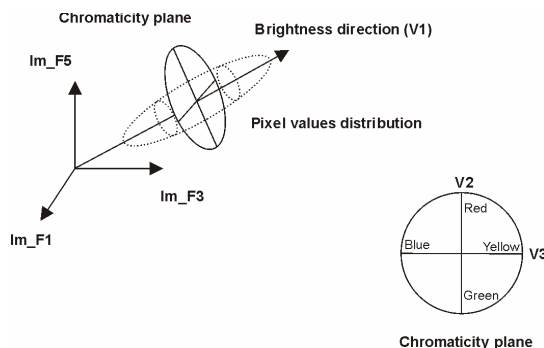


Figure 4. PCA modified method

Finally, another simple empirical method included in the second group was studied. Using this method, an optimization process maximizing the color difference

between samples was performed. Due to the great number of free parameters and the associated high computational cost, we consider that the  $R_{NIR}$ ,  $G_{NIR}$  and  $B_{NIR}$  signals must be linear combinations of the five monochrome images and that the coefficients of the combinations must take one of two possible values: 0.1 or 0.9.

## 2. Calibration of the Visualization Device

Once the color representation used to transform the information included in the NIR into visible information is defined, the  $R_{NIR}$ ,  $G_{NIR}$  and  $B_{NIR}$  signals obtained must be displayed on a visualization device; in our case, a conventional CRT monitor. Depending on the characteristics of the device used, that is, its gamut mapping, the samples may appear to be pseudocolored differently. In order to prevent this, we can previously transform these signals, taking into account the color calibration of the specific device used. Thus, the final colors represented on the screen will not depend on the monitor used. The process used to transform the signals is summarized in Figure 5, below.

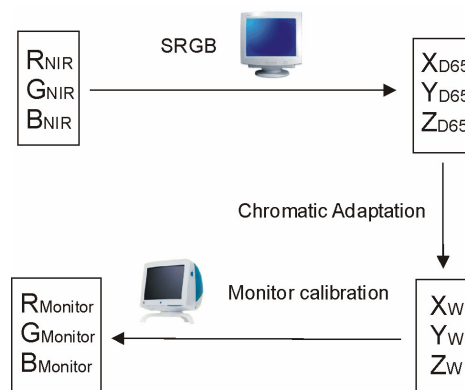


Figure 5. Diagram showing the transformation of the  $R_{NIR}$ ,  $G_{NIR}$  and  $B_{NIR}$  signals

First of all, the  $R_{NIR}$ ,  $G_{NIR}$  and  $B_{NIR}$  signals were transformed into the tristimulus values  $X_{D65}$ ,  $Y_{D65}$  and  $Z_{D65}$ , taking into account the standard space sRGB.<sup>6</sup> The CIE sRGB space had been defined using an average of conventional CRT monitors. The reference white used in this space was the illuminant D65, with a luminance of 100 cd/m<sup>2</sup>. On the basis of this first transformation, we considered that the  $R_{NIR}$ ,  $G_{NIR}$  and  $B_{NIR}$  signals corresponded to the signals that would be associated with the channels of the standard monitor of the sRGB space. However, depending on the primaries of the monitor that is actually used, the reference white may not be the illuminant D65. For this reason, chromatic adaptation is needed<sup>7</sup>, because it allows a color to be conveniently transformed so that it gives the same chromatic sensation under the illuminant D65 as under the new reference white ( $X_W$ ,  $Y_W$  and  $Z_W$ ). With these new tristimulus values and the parameters of the color calibration of the monitor used, it is possible to obtain the final digital values that must be associated with the channels of the monitor used ( $R_{Monitor}$ ,  $G_{Monitor}$  and  $B_{Monitor}$ ). The method we used to perform the calibration was the standard GOG (Gamma, Offset, Gain) method defined by the CIE.<sup>8,9</sup>

In this study, we used a conventional CRT monitor (Hansol) to perform the visualization. The contrast and brightness of the monitor had been adjusted in order to obtain a luminance similar to that of the standard monitor ( $105.4 \text{ cd/m}^2$ ). The characteristics of the primaries can be seen in Figure 6 and Table 1.

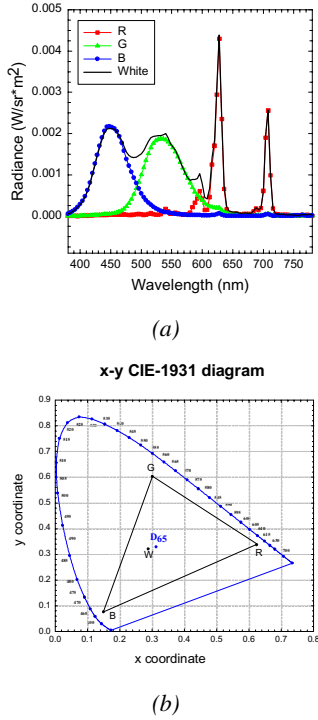


Figure 6. (a) Spectral emission of the primaries and white of the monitor and (b) chromaticity coordinates

Table 1. Chromaticity coordinates and luminance of the primaries and white of the monitor

	x	y	L (Cd/m <sup>2</sup> )
R	0.6246	0.3369	19.50
G	0.3016	0.6015	79.59
B	0.1499	0.0753	11.71
White	0.2884	0.3210	105.4

Using the information of the primaries and the tone reproduction curves of the monitor (Figure 7), which relate the relative luminance of the primaries to the normalized digital outputs, the GOG model provides the parameters of the color calibration (Table 2).

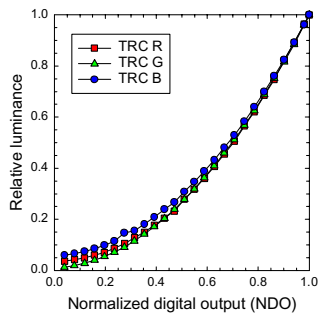


Figure 7. Tone reproduction curves of the monitor

Table 2. Parameters of calibration (GOG) of the monitor

	g	o	γ
R	0.8088	0.1912	2.5170
G	0.9334	0.0666	2.0933
B	0.6938	0.3062	2.8093

The overall transformation process of the signals is described by the following expressions:

#### sRGB

$$k_{NIR} \equiv \left( \frac{L}{L_{max}} \right)_k = (g_k \cdot NDO_{k_{NIR}} + o_k)^{\gamma_k} \quad (5)$$

$$\begin{bmatrix} X_{D65} \\ Y_{D65} \\ Z_{D65} \end{bmatrix} = \begin{bmatrix} 41.23 & 35.76 & 18.05 \\ 21.26 & 71.52 & 7.22 \\ 1.93 & 11.92 & 95.06 \end{bmatrix} \cdot \begin{bmatrix} R_{NIR} \\ G_{NIR} \\ B_{NIR} \end{bmatrix} \quad (6)$$

where  $k=R, G$  and  $B$ ,  $g_k=0.95$ ,  $o_k=0.05$  and  $\gamma_k=2.40$  (sRGB standard monitor), and  $X_{D65}, Y_{D65}, Z_{D65}$  in  $\text{cd/m}^2$ .

#### Chromatic Adaptation

$$\begin{bmatrix} X_W \\ Y_W \\ Z_W \end{bmatrix} = 105.4 \text{ cd/m}^2 M_{adapt} \frac{1}{100 \text{ cd/m}^2} \begin{bmatrix} X_{D65} \\ Y_{D65} \\ Z_{D65} \end{bmatrix} \quad (7)$$

$$M_{adapt} = \begin{bmatrix} 0.9423 & -0.0307 & 0.0307 \\ -0.0437 & 1.0287 & 0.0118 \\ 0.0038 & -0.0048 & 1.1185 \end{bmatrix} \quad (8)$$

#### Monitor Calibration

$$\begin{bmatrix} R_{Monitor} \\ G_{Monitor} \\ B_{Monitor} \end{bmatrix} = \begin{bmatrix} 0.0377 & -0.0180 & -0.0055 \\ -0.0093 & 0.0172 & 0.0001 \\ 0.0003 & -0.0015 & 0.0084 \end{bmatrix} \cdot \begin{bmatrix} X_w \\ Y_w \\ Z_w \end{bmatrix} \quad (9)$$

$$NDO_{k_{Monitor}} = \frac{k_{Monitor}^{1/\gamma_k} - o_k}{g_k} \quad \text{if } k_{Monitor} > 0.0031308$$

$$NDO_{k_{Monitor}} = 12.92 \cdot k_{Monitor} \quad \text{if } k_{Monitor} \leq 0.0031308 \quad (10)$$

At very low levels, the tone reproduction curves fit a linear function better. In these special cases, the transformation used is the same as that corresponding to the sRGB space.

#### Results

Once the color images were obtained and conveniently transformed according to the monitor used, we were able to quantify the results in terms of colorimetric discrimination. In order to evaluate the color contrast in the pseudocolored images of the twenty-five textile samples, we used the following parameters:

### Pseudocolor Difference

$$\Delta \tilde{E} = \left[ \left( \Delta(ND_{R\text{Monitor}}) \right)^2 + \left( \Delta(ND_{G\text{Monitor}}) \right)^2 + \left( \Delta(ND_{B\text{Monitor}}) \right)^2 \right]^{1/2} \quad (11)$$

This parameter gives information related to the color difference but also to the luminance difference. This parameter is calculated with the digital signals of the channels of the monitor.

### RG-RB-GB Contrast

$$\begin{aligned} C_{RG} &= \left| \frac{ND_{R\text{Monitor}} - ND_{G\text{Monitor}}}{ND_{R\text{Monitor}} + ND_{G\text{Monitor}}} \right| \\ C_{RB} &= \left| \frac{ND_{R\text{Monitor}} - ND_{B\text{Monitor}}}{ND_{R\text{Monitor}} + ND_{B\text{Monitor}}} \right| \\ C_{GB} &= \left| \frac{ND_{G\text{Monitor}} - ND_{B\text{Monitor}}}{ND_{G\text{Monitor}} + ND_{B\text{Monitor}}} \right| \\ C_{TOT} &= C_{RG} + C_{RB} + C_{GB} \end{aligned} \quad (12)$$

This parameter gives an idea of the tones or coloration degree included in the images. The smaller the parameter, the grayer the samples in the pseudocolored image. This parameter is calculated with the digital signals of the channels of the monitor.

### CIELAB Color Difference

$$\Delta E = \left[ (\Delta L)^2 + (\Delta a)^2 + (\Delta b)^2 \right]^{1/2} \quad (13)$$

This parameter was measured using the monitor and a PR-650 spectroradiometer.

Several examples of the pseudocolored images obtained with the different methods are shown in Figure 8. The numeric results for the examples presented are summarized in Table 3.

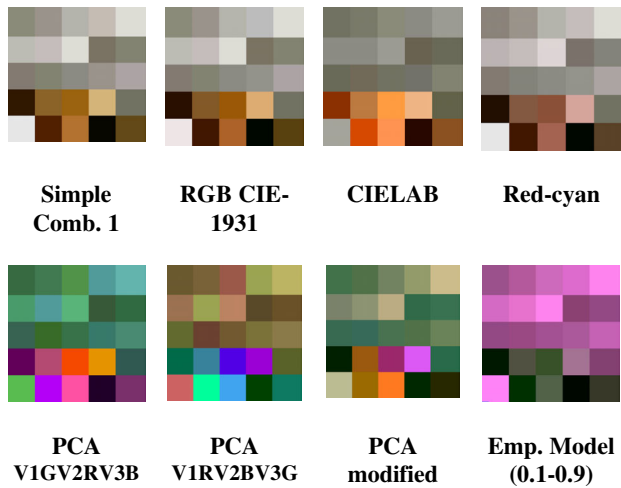


Figure 8. Examples of the final pseudocolored images

The best results in terms of visual discrimination and contrast levels are achieved by using the PCA decorrelation model. In this method, the RG-RB-GB

contrasts and the CIELAB color differences have maximum values. Unlike these two parameters, the maximum values for the pseudocolor difference are obtained with the simple combination, the RGB CIE-1931 and the empirical models. As previously stated, these parameters do not only account for the color difference but also for the difference in luminance. As shown in Figure 8, these methods provide images with a uniform tone but with many shades of gray. Depending on whether we want to simulate the vision of the human eye or to discriminate samples, two different methods are possible. Because of the high correlation of the spectral bands in the NIR region, the images obtained using the first type of method are often neutral. If decorrelation methods are used instead, it is easier to discriminate between the samples.

Table 3. Parameters of quantification of the color differences (mean and standard deviation of the twenty-five samples)

METHOD	Pseudocolor difference	RG-RB-GB contrast	CIELAB color difference
Simple Comb. 1	111.38±76.79	0.2499±0.3787	30.76±19.22
RGB CIE-1931	115.55±79.69	0.2516±0.3833	32.36±20.31
CIELAB	83.06±57.15	0.3360±0.5404	29.99±21.68
RED-CYAN	109.40±78.71	0.1309±0.1980	27.75±18.66
PCA V1GV2RV3B	104.94±59.70	0.6526±0.5553	59.08±38.93
PCA V1RV2BV3G	104.94±59.70	0.6526±0.5553	50.83±39.42
PCA modified	104.33±63.97	0.5110±0.5340	39.97±30.50
Emp. Model (0.1-0.9)	125.60±89.02	0.5275±0.2496	41.55±29.76

### Conclusion

For this study, we developed a color visualization system for multispectral images belonging to the NIR region of the spectrum. The process was divided into two stages: 1) pseudocolorimetry definition, for which different color representations were proposed in order to obtain the signals  $R_{NIR}$ ,  $G_{NIR}$  and  $B_{NIR}$ , which are considered to be the pseudocolors of the samples, and 2) calibration of the visualization device, in which the last signals were conveniently transformed in order to obtain similar chromatic sensations with any visualization device that could be used. For the first stage, several pseudocoloring methods were proposed: some of these simulated the color vision of the human eye and others were based on decorrelation methods (PCA). For the second stage, a GOG model was used to calibrate a CRT monitor on which the color images were displayed. Finally, the pseudocolored images were numerically analyzed in terms of color differences. The PCA method provided the best results in terms of discrimination between the samples. On the other hand, the simple combination and the RGB CIE-1931 model offer a better simulation of the vision of the human eye, although only in the NIR region.



## Acknowledgements

This research was supported by the Ministerio de Ciencia y Tecnología (Spain) under grant DPI2002-00118. M. Vilaseca would like to thank the Generalitat de Catalunya for the PhD grant she has received.

## References

1. M. Vilaseca, J. Pujol and M. Arjona, Spectral-reflectance reconstruction in the near-infrared region by use of conventional charge-coupled-device camera measurements, *Applied Optics* 42 10, 1788-1797 (2003).
2. D. Scribner, P. Warren, J. Schuler, M. Satyshur, and M. Kruer, Infrared color vision: an approach to sensor fusion, *Optics & Photonics News* 9 8, 27-32 (1998).
3. J. M. Artigas, P. Capilla, A. Felipe and J. Pujol, *Óptica Fisiológica: Psicofísica de la visión*, McGraw-Hill Interamericana de España, Madrid, 1995.
4. M. D. Fairchild, *Color Appearance Models*, Addison-Wesley, Reading, Massachusetts, 1998.
5. R. C. Gonzalez, R. E. Woods, *Digital image processing*, Addison-Wesley Longman, Massachusetts, 1993.
6. J. M. Artigas, P. Capilla and J. Pujol, *Tecnología del color*, Publicacions de la Universitat de València, València, España, 2002.
7. R.S. Berns, *Principles of color technology*, John Wiley and Sons, New York, 2000.
8. R. S. Berns, *Methods for characterizing CRT displays*, *Displays* 16 4, 173-182 (1995).
9. CIE 122-1996, *The relationship between digital and colorimetric data for computer-controlled CRT displays*.

## Biography

**Meritxell Vilaseca** completed her BS Degree in Physics at the Autonomous University of Barcelona in 2000. She completed her Degree in Optics and Optometry at the Technical University of Catalonia in 1996. She is currently enrolled in the PhD program in Optical Engineering at the Technical University of Catalonia. Her work focuses on multispectral imaging, camera calibration and characterization, industrial colorimetry, color management and imaging. E-mail: mvilasec@oo.upc.es